ELSEVIER

Available online at www.sciencedirect.com
SCIENCE DIRECT

Journal of Crystal Growth 251 (2003) 367–371

JOURNAL OF CRYSTAL GROWTH

www.elsevier.com/locate/jcrysgro

1.5 μm GaInNAs(Sb) lasers grown on GaAs by MBE

Seth Bank[a,*], Wonill Ha[a], Vincent Gambin[a], Mark Wistey[a], Homan Yuen[a], Lynford Goddard[a], Seongsin Kim[b], James S. Harris Jr.[a]

[a] *Solid State and Photonics Lab., CISX B113-3, Via Ortega, Stanford University, Stanford, CA 94305 USA*
[b] *Agilent Technologies Inc., San Jose, CA 95131 USA*

Abstract

We demonstrate the first 1.5 μm GaInNAsSb laser grown on GaAs. It exhibits much improved threshold current density as compared with previously reported GaInNAs lasers at 1.52 μm. A 1.465 μm laser with far superior performance is also demonstrated. This device exhibits a pulsed threshold current density of 930 A/cm^2 per quantum well, a differential quantum efficiency of 0.30 W/A (both facets), an external quantum efficiency of 35%, and peak power above 70 mW. Additionally, the use of antimony allows for a decrease in the bandgap out to 1.6 μm, while still preserving luminescence efficiency as compared to 1.3 μm GaInNAs material.
© 2003 Elsevier Science B.V. All rights reserved.

PACS: 78.55.Cr; 78.66.Fd; 78.60.Fi

Keywords: A1. Photoluminescence; A3. Molecular beam epitaxy; A3. Quantum wells; B1. Nitride-arsenides; B2. Semiconducting quaternary alloys; B3. Laser diodes

1. Introduction

The proliferation of optical fiber communications has led to a high demand for low cost, 1.3–1.6 μm lasers that are essential for the rapid expansion of optical metro area networks (MANs). The requirements for these lasers are broad operating temperature range (−10°C to 90°C), emission spectra over 1.3−1.6 μm, and moderate power (> 10 mW). There is also a significant interest in higher power lasers, at similar wavelengths, as pumps for Raman amplifiers to improve available bandwidth. Heretofore, InP-based lasers have been used for all these applications, but they have serious shortcomings that greatly hinder their ability to cover the 1.3–1.6 μm wavelength range [1], both for low cost vertical-cavity surface-emitting lasers (VCSELs) and high-power Raman pumps. InP-based VCSELs have been demonstrated with excellent performance, but at the price of extensive back-end processing [2].

The demand for these high performance and cost effective near infrared laser sources around 1.3 μm provided the initial impetus for studying the dilute nitrides. Grown on GaAs, GaInNAs offers many advantages in comparison to current InP-based materials, including well-developed GaAs processing techniques, inexpensive substrates, and superior DBR (Distributed Bragg

*Corresponding author. Tel.: +1-650-7258313; fax: +1-650-7234659.

E-mail address: sbank@stanford.edu (S. Bank).

0022-0248/03/$ - see front matter © 2003 Elsevier Science B.V. All rights reserved.
doi:10.1016/S0022-0248(02)02446-6

Reflector) mirror technology available for VCSELs [3,4]. Laser diodes with GaInNAs active layers have shown prospective characteristics, including low threshold current density, high temperature CW operation, and high T_0 in the wavelength range of 1.1–1.3 μm. Based on these results, efforts were undertaken to push the material to longer wavelengths to reach the conventional fiber-communication wavelength range centered at 1.55 μm. The inability to push GaInNAs lasing wavelength beyond ~1.4 μm, led this group to study surfactant mediated growth using antimony during molecular beam epitaxy (MBE) growth. The use of low fluxes $\sim 10^{-8}$ Torr showed the ability to increase indium content in the quantum wells (QWs). Additional increase of the flux led to antimony incorporation and a further redshift of the material. The incorporated antimony allowed more indium incorporation compounding the redshift. Additional bandgap reduction is attributed to the significant bowing of nitride-antimonide alloys predicted from $k{\cdot}p$ methods [5]. We present results from photoluminescence (PL) measurements and two sets of in-plane lasers using GaInNAsSb QWs surrounded by GaNAsSb barriers. Post-annealed PL spectra with luminescence peaks out to 1.6 μm were observed without serious degradation of luminescence efficiency and crystal quality. In-plane lasers from the samples yielded lasers at 1.46 μm with pulsed threshold current density of 930 A/cm^2 per QW, operation out to 90°C, and maximum output power >70 mW. Longer wavelength lasers were grown and found to exhibit lasing beyond 1.49 μm. This laser exhibits improved threshold current density as compared to the first GaInNAs laser to reach 1.5 μm [6]. These proof of principle laser results show that GaInNAsSb QWs are an excellent active layer material for high output power edge-emitting lasers and lower power VCSELs that will serve as amplifiers and sources in future generations of long haul optical networks.

2. Molecular beam epitaxy (MBE) growth

The samples used in this study were prepared by solid source MBE (Varian Gen II system). All column III elements were supplied by elemental solid source effusion. Nitrogen was provided by an SVT RF nitrogen plasma mounted directly on a 4.5″ source port. The other column V sources, arsenic and antimony, were supplied with standard cracking cells. The growth chamber was kept under UHV (background pressure $\sim 10^{-10}$ Torr) by a cryo-pump and an ion pump to minimize impurities incorporated. To ensure the growth rate of each source, several beam equivalent pressure measurements were taken before growth with a Bayard–Alpert type pressure gauge. All samples with nitrogen incorporation were grown with relatively high arsenic overpressure of ~20 times the total group III flux. The nitrogen concentration in the epitaxial layers has been found to be controlled by the group III growth rate [7]. GaAs substrates were cleaned at 350°C for 1 h in a separate chamber before loading into the growth chamber. To remove the native oxide from the surface prior to buffer layer growth, the substrate was cleaned at 10°C above the deoxidation temperature for 10 min under an arsenic overpressure. The plasma source was ignited 10 min prior to active layer growth to minimize unwanted nitrogen background and the related ion damage. RF power and nitrogen flow rate were set to 300 W and 0.25 sccm, respectively, and the reflected power was kept at minimum with a RF matching network. The growth temperature was monitored by pyrometer as well as oxide desorption prior to growth. To prevent nitrogen and indium desorption, the active layer was grown at 415°C.

3. Photoluminescence experiments

The longest wavelengths achievable with high indium content InGaAs are limited by low critical thicknesses caused by a large lattice mismatch. The use of nitrogen helps to shrink the bandgap while reducing the strain due to the large bowing parameter between bandgap and lattice constant. However, nitrogen lowers optical efficiency due to the introduction of nitrogen-related non-radiative recombination centers. As a result, it is preferable to extend the wavelength of the material by introducing the minimum nitrogen that allows a

sufficient amount of indium. The limiting mechanism is the same in this case as it was for pure InGaAs; high interface stress causes islanding in order for the film to satisfy Young's equation. This is illustrated in Fig. 1, which shows the highest 1.3 μm PL achieved by this group (31% indium). Extending the wavelength a bit further by adding 4% more indium, along with sufficient nitrogen, degrades the luminescence by three orders of magnitude.

The desire to maintain 2-D growth at higher indium concentrations has led to much research on surfactant-assisted growth using antimony [8–10]. The reduction in surface free energy afforded by the antimony flux of 7.2×10^{-8} Torr allowed the growth of QWs with 38% indium without significant reduction in luminescence intensity. The PL peak was found to be ~1.38 μm. Using a higher antimony flux of 1.2×10^{-7} Torr and 39% indium, a peak PL at 1.5 μm was demonstrated (Fig. 1). This sample preserved ~80% of the intensity of the 1.38 μm sample. Increasing the antimony flux further to 1.4×10^{-7} Torr resulted in a PL peak at 1.6 μm but with an intensity decrease of more than an order of magnitude (Fig. 1). It is expected that by optimizing the QW composition, a greater portion of the luminescence can be maintained between 1.3 and 1.6 μm.

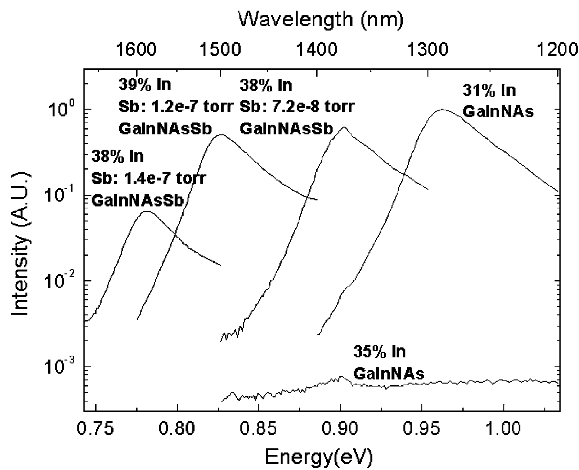

Fig. 1. PL results for various antimony fluxes relative to the best 1.3 μm peak achieved.

In all cases, the luminescence reported in Fig. 1 is that from the best annealing time and temperature. Typically, the optimal anneal is within the range 720–820°C for 1–3 min. The annealing effects are typically an increase in the luminescence intensity and a monotonic blueshift. The initial improvement in PL intensity is attributed to the annealing of crystalline imperfections such as point defects and arsenic antisites. The blueshift has been attributed to many causes including nitrogen outdiffusion, nitrogen nearest neighbor rearrangement, and Ga/In interdiffusion [4,11,12]. It is likely that the cause is a combination of these (and maybe other) causes where the relative

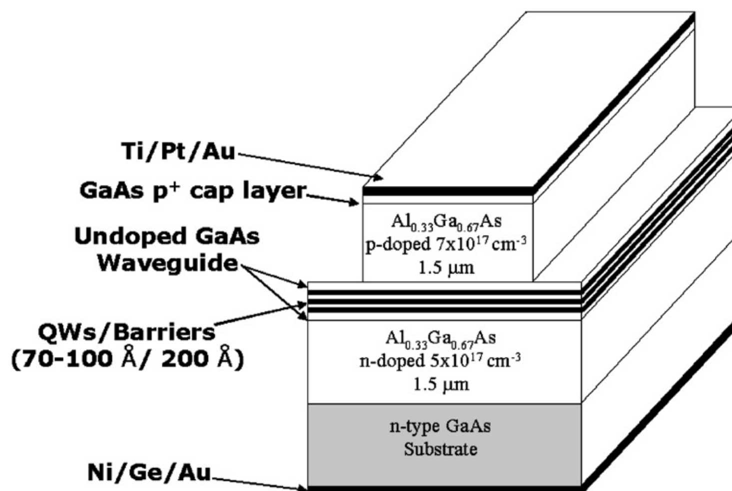

Fig. 2. Laser structure used for this study.

importance of each depends on the growth conditions and compositions.

4. Device structure and fabrication

The separate confinement heterojunction (SCH) laser diode structures were grown on (1 0 0) *n*-type GaAs substrate and are shown schematically in Fig. 2. The active region consists of GaInNAsSb quantum wells separated by 200 Å GaNAsSb barriers. The active region is embedded in the middle of a 1200 Å thick undoped GaAs waveguide. The active layer was sandwiched between 1.5 μm Si doped ($5 \times 10^{17}\,cm^{-3}$) n-type $Al_{0.33}Ga_{0.67}As$ and 1.5 μm Be doped ($7 \times 10^{17}\,cm^{-3}$) p-type $Al_{0.33}Ga_{0.67}As$ cladding layers. Above the claddinf was a 500 Å p^{+} ($1 \times 10^{19}\,cm^{-3}$) GaAs cap layer for contacting. The wafer was removed from the chamber and annealed ex situ by rapid thermal annealing (RTA) at the optimum temperature, dependent on the group III and group V compositions, to improve material quality [13]. The optimal annealing conditions for the highest PL intensity and smallest FWHM and are typically in the range 760–820°C for 1–2 min. We also found that growth of the top cladding layer provides in situ annealing and results in a change in the optimal ex situ annealing temperature with respect to PL samples. In general, the optimal anneal for lasers is generally 60°C below that of PL samples. Based on this, the laser diodes were annealed at 780°C for 1 min.

The ridge waveguide laser process flow consisted of lithographic patterning of the top Ti/Pt/Au contacts. Mesas were defined by a self-aligned reactive ion etch (RIE) through the top cladding layer. A dilute wet etch was utilized following the RIE etch to improve sidewall roughness and reduce optical scattering losses. The substrate was lapped and polished down to 100 μm for better thermal conduction and manual cleaving convenience. The thinned substrates were evaporated with Ni/Ge/Au and alloyed at 430°C. Facets were then manually cleaved resulting in a variety of cavity lengths. No facet coatings were applied.

For measurement, devices were placed p-side up on a temperature-controlled copper chuck without the use of solder, conductive epoxy, or active cooling. Light output was measured using a calibrated broad area InGaAs photodiode and spectral data was taken with an optical spectrum analyzer.

5. Results

Based on the promising PL results, two sets of edge-emitting lasers were fabricated. A ridge waveguide laser was grown under the same conditions as the sample with antimony flux of 7.2×10^{-8} Torr. This sample was grown with three 70 Å GaInNAsSb QWs and 200 Å GaNAsSb barriers, GaAs waveguides and top and bottom AlGaAs cladding layers. Fig. 3(a) shows the light output power as a function of injection current. As shown in Fig. 3(b), the laser diodes exhibit luminescence at 1.465 μm with a maximum power of exceeding 70 mW from a 5 μm wide stripe. The minimum threshold current density was 2.8 kA/

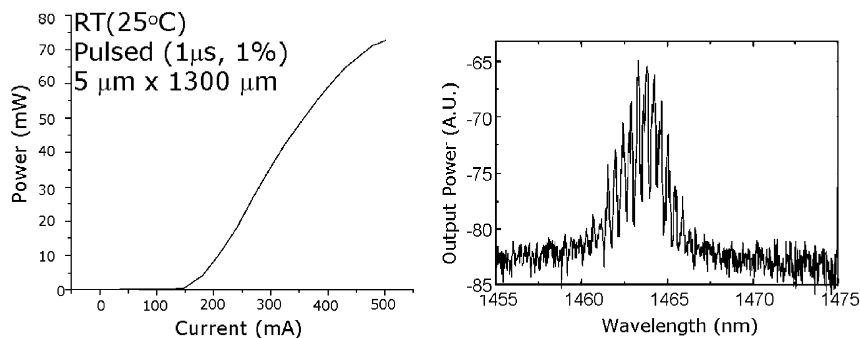

Fig. 3. (a) $L-I$ curve and (b) spectrum for the laser with antimony flux of 7.2×10^{-8} Torr.

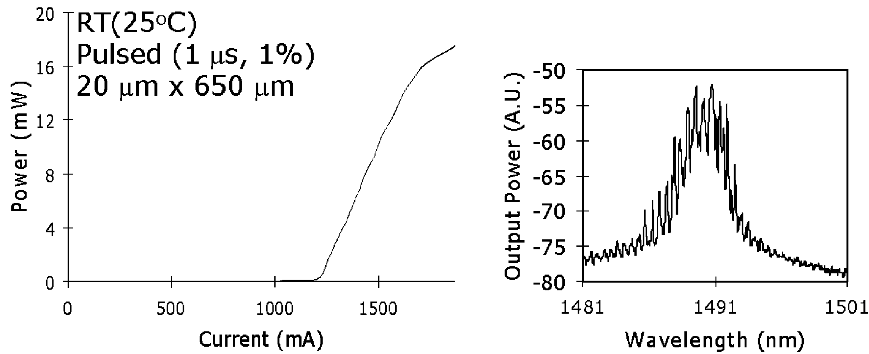

Fig. 4. (a) $L\!-\!I$ curve and (b) spectrum for the laser with antimony flux of 1.4×10^{-7} Torr.

cm^2, which is 930 A/cm^2 per QW. This laser showed a differential quantum efficiency, η_d, of 0.30 W/A (both facets) and an external quantum efficiency, η_e, of 35%. To our knowledge, this is the lowest threshold current density for lasers beyond 1.4 μm on a GaAs substrate.

The second laser sample was grown with an antimony flux of 1.4×10^{-7} Torr. From critical thickness concerns, the device was grown with only a single 100 Å wide QW. As shown in Fig. 4, the laser exhibits lasing out to 1.49 μm. The device performance is degraded compared to the previous one at 1.46 μm as the threshold current density was found to be 18.8 kA/cm^2. The high current density is probably a result of under annealing coupled with the small overlap between the guided mode and the thin active layer. Additionally, the devices had shorter wavelength emission than that of the PL samples grown under the same condition. This may be caused by the unvalved antimony source used for this growth, since the antimony flux may vary over the course of the growth. Moreover, oval defects were readily visible on the surface and reduced device-to-device uniformity. Higher performance lasers are expected from further optimization of the indium, nitrogen, and antimony related growth conditions.

6. Conclusion

We have demonstrated proof-of-principle results from a new material combination of GaInNAsSb/GaNAsSb (QW/barrier). Using antimony, it is possible to extend the wavelength attainable with GaInNAs without catastrophic degradation of the PL intensity. Peak PL of 1.6 μm is demonstrated from a QW grown with an antimony beam equivalent pressure of 1.4×10^{-7} Torr. Lasers grown from QWs with long wavelength PL resulted in devices with lasing at 1.465 μm. Peak power >70 mW is observed from a 5 μm wide stripe. This device shows a threshold current density of 930 A/cm^2 per quantum well, η_d of 0.30 W/A (both facets), and η_e of 35%. Additionally, a laser at 1.49 μm was also demonstrated but with drastically increased threshold current density. We believe that GaInNAsSb active layers are ideally suited for use in broad bandwidth communication sources and Raman amplifier pumps to service the S, C, and L bands.

References

[1] A.F. Phillips, et al., IEEE J. Select. Topics Quantum Electron. 5 (1999) 301.
[2] G. Boehm, et al., MBE Conference, 2002.
[3] M. Kondow, et al., IEEE J. Select. Topics Quantum Electron. 3 (1997) 719.
[4] J.S. Harris Jr., IEEE J. Select. Topics Quantum Electron. 6 (2000) 1145.
[5] B.N. Murdin, et al., Appl. Phys. Lett. 11 (2001) 1568.
[6] M. Fischer, et al., Electron. Lett. 36 (2000) 1208.
[7] J.S. Harris, Semicond. Sci. Tech. 17 (2002) 880.
[8] X. Yang, et al., Appl. Phys. Lett. 74 (1999) 2337.
[9] H. Shimizu, et al., Electron. Lett. 36 (2000) 1701.
[10] X. Yang, et al., Appl. Phys. Lett. 78 (2001) 4068.
[11] P.L. Klar, et al., Phys. Rev. B 64 (2001) 64.
[12] O.M. Khreis, et al., J. Appl. Phys. 84 (1998) 232.
[13] T. Kitatani, et al., J. Crystal Growth 209 (2000) 345.